第 31卷 第 3期　　焊 接 学 报　　Vol.31 No.3
2010年 3月　　TRANSACTIONS OF THE CHINA WELDING INSTITUTION　　March 2010

铝合金脉冲激光焊 Mg元素烧损行为及接头硬度分布

牛锐锋，　林冰华，　王亚妮，　杨兴飞
（西安理工大学 材料科学与工程学院，西安　710048）

牛锐锋

摘　要：采用 Nd:YAG脉冲激光对 1 mm厚 5A05铝合金板进行焊接，结合激光焊物理过程，研究和分析了焊接工艺参数（脉冲能量、脉冲宽度、焊接速度和离焦量）对 Mg元素烧损和焊缝熔深的影响，以及焊缝中 Mg元素含量的变化和接头的硬度分布．结果表明，Mg元素烧损受熔池搅拌作用的影响，随搅拌作用增强和焊缝熔深的增加，焊缝中 Mg元素烧损率减小；受 Mg元素含量和冷却速度影响，焊接接头硬度在熔合线附近具有最大值，在焊缝中从表面到熔池底部硬度先减小再增大．

关键词：脉冲激光焊；Mg元素烧损；铝合金；显微硬度
中图分类号：TG456.7　　文献标识码：A　　文章编号：0253－360X(2010)03－0081－04

0　序　言

激光焊作为一种新型焊接技术，具有能量密度高、焊接热输入低、焊接速度快、热影响区小等优点[1,2]，在焊接铝合金方面有较大的优势．近年来，铝合金激光焊接受到了国内外学者的关注，对有关理论和工艺问题进行了诸多研究，工作主要涉及激光焊时铝合金的熔化特性、等离子体吸收效应、焊接过程中气孔和裂纹缺陷的成因等方面[3－6]．

结构用铝合金中通常含有 Mg，Zn，Li等低沸点元素，在激光焊接时这些元素会因蒸发而损失，造成焊缝金属合金元素含量不足，接头性能降低．而有关激光焊接参数对合金元素烧损影响方面的研究还鲜见报道．文中以 5A05铝合金为对象，结合激光焊物理过程，研究了脉冲激光焊时焊缝中 Mg元素的烧损行为，并对接头硬度进行了测定和分析．

1　试验方法

试验材料为 1.0 mm厚的 5A05铝合金板，其化学成分见表 1．试样尺寸为 80 mm×40 mm×1 mm．焊接设备为 JHM—1GY—500B型多功能激光加工机，激光源为 Nd:YAG脉冲激光器．用氩气作为保护气体，自熔焊方法制备焊接接头．焊接完成后，切取焊缝横断面金相试样，用 OXford INCA型高性能 X射线能谱仪对焊缝中 Mg元素分布进行线扫描和点采样．用 TUKON 2100型显微硬度计测试焊缝及焊接接头的显微硬度分布．

收稿日期：2008－10－06

表 1　5A05铝合金的化学成分（质量分数，%）
Table 1　Chemical composition of 5A05 aluminum alloy

Cu	Mn	Si	Fe	Zn	Mg	杂质	Al
0.1	0.4	0.5	0.5	0.2	5.5	0.1	余量

2　结果与分析

2.1　熔池内 Mg元素分布

在激光焊接 5A05铝镁合金时，由于 Mg元素的沸点（1 380 K）低，所以焊接过程中必将有一部分 Mg元素蒸发烧损，造成 Mg元素在焊缝金属中的缺失．采用 X射线能谱仪对焊缝中元素分布进行线扫描和点采样分析，扫描和采样位置如图 1所示．图 2为焊缝厚度方向 Al，Mg元素的能谱分析结果，从图2

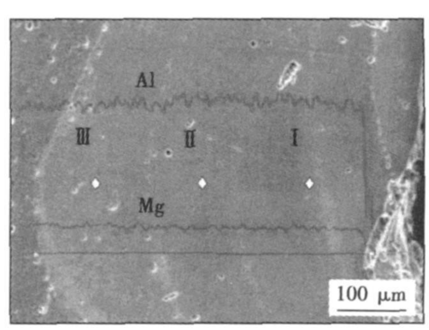

图 1　焊缝能谱采样部位
Fig.1　EDS testing area

中可看出,从熔池底部到焊缝表面 Mg元素含量有下降趋势,而 Al元素含量变化不大. 表 2是母材及焊缝不同部位 Mg元素含量的能谱分析结果. 由表 2可知, 5A05铝合金焊缝中的 Mg元素含量均低于母材; 在焊缝上部 Mg元素的绝对损失量达 1.83%,中部为 1.52%,下部仅为 0.71%. 由此可见, 5A05铝合金激光焊焊缝中存在 Mg元素的烧损现象,且在焊缝上部和中心区域表现较为明显.

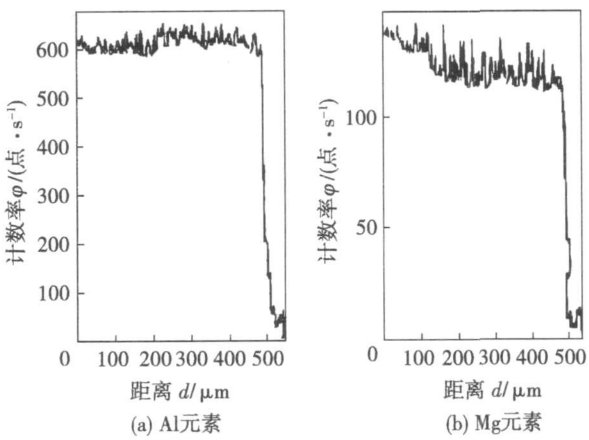

图 2 铝和镁元素从焊缝底部到表面的分布

Fig. 2 Distribution of Al and Mg elements in welding joint

表 2 母材及焊缝各部位 Mg元素含量(质量分数, %)

Table 2 Mg content in EDS testing area

母材	焊缝上部(Ⅰ)	焊缝中部(Ⅱ)	焊缝下部(Ⅲ)
5.5	3.67	3.98	4.79

2.2 焊接参数对 Mg元素烧损和熔深的影响

选用 4因素 3水平正交试验考察脉冲激光焊接时焊接速度、离焦量和决定脉冲能量的电流、脉冲宽度对 Mg元素烧损和熔深的影响. 用烧损率 ϕ 表征 Mg元素的烧损情况,其计算公式为

$$\phi = \frac{W_1 - W_2}{W_1} \times 100\%$$

式中: W_1 为母材中 Mg元素的质量分数; W_2 为焊缝中 Mg元素的质量分数 (均取自焊缝中心线上距焊缝表面 0.1 mm处).

正交试验因子计划表及结果见表 3、表 4. 由表 4可得焊接工艺参数对 Mg元素烧损率和熔深的影响趋势极差分析图 (图 3). 由图 3可知,脉冲宽度、焊接速度、离焦量和电流对 Mg元素烧损和焊缝熔深均有较大影响,各参数对 Mg元素烧损率和熔深的影响大体相反. 随着电流和脉冲宽度的增加,熔深增大, Mg元素烧损减少;而随着焊接速度和离焦量的增大,熔深减小, Mg元素烧损增加.

表 3 正交试验因子水平表

Table 3 Orthogonal design factor levels

水平	脉冲宽度 τ/ms	焊接速度 υ/(mm·s⁻¹)	离焦量 F/mm	电流 I/A
1	2.7	1.5	10	193
2	2.5	3.0	8	195
3	3.0	2.5	12	191

表 4 正交试验实施计划及结果

Table 4 Orthogonal experiment scheme and experimental data

试验号	脉冲脉宽 τ/ms	焊接速度 υ/(mm·s⁻¹)	离焦量 F/mm	电流 I/A	试验结果 熔深 h/mm	试验结果 烧损率 ϕ(%)
1	2.7	1.5	10	193	0.546	42.4
2	2.7	3.0	8	195	0.559	44.0
3	2.7	2.5	12	191	0.268	55.1
4	2.5	1.5	8	191	0.585	42.0
5	2.5	3.0	12	193	0.325	55.6
6	2.5	2.5	10	195	0.364	44.2
7	3.0	1.5	12	195	0.338	32.5
8	3.0	3.0	10	191	0.325	51.3
9	3.0	2.5	8	193	0.715	33.3

2.3 焊接参数对 Mg元素烧损影响的机理分析

脉冲激光焊时,金属表面被迅速加热,发生熔化和汽化. 逸出的金属蒸气以一定的速度离开熔池表面,并产生一个附加压力反作用于熔化金属,使熔池金属表面向下凹陷,在激光光斑下产生一个小凹坑. 由于工件和光束之间有相对运动,凹坑熔化前沿直接处于激光束下方,金属温度高、蒸发快,而后熔化边沿附近的金属温度低、蒸发慢,由此产生蒸气反作用压强差,导致熔化金属由前向后流动,客观上起到了对熔池的搅拌作用. 此外,凹坑附近具有较大的温度梯度. 根据 Marangoni效应[7],不均匀表面温度将引起表面张力的不均匀分布,从而在熔池上表面存在着表面张力梯度. 表面张力梯度促使熔池金属从表面张力低的部位流向表面张力高的部位. 由于熔池边缘附近温度较低,表面张力较大,而熔池中心温度较高,表面张力较小,所以熔池中心附近的金属液体被拉向熔池边缘,使得熔池表面的液体从中心向外流动. 在熔池中心处,由于要不断地对表面流出的液体进行补充,因此液体金属将由下向上流动. 这样就形成了熔池金属的循环流动,产生了对熔池的搅拌作用,能将熔池底部的物质更多的带到熔池上部,弥补上部由于烧损而含量减少的合金元素. 虽然搅拌作用增强导致焊缝整体 Mg元素烧损加剧,但在一定程度上可弥补熔池上部元素的烧损.

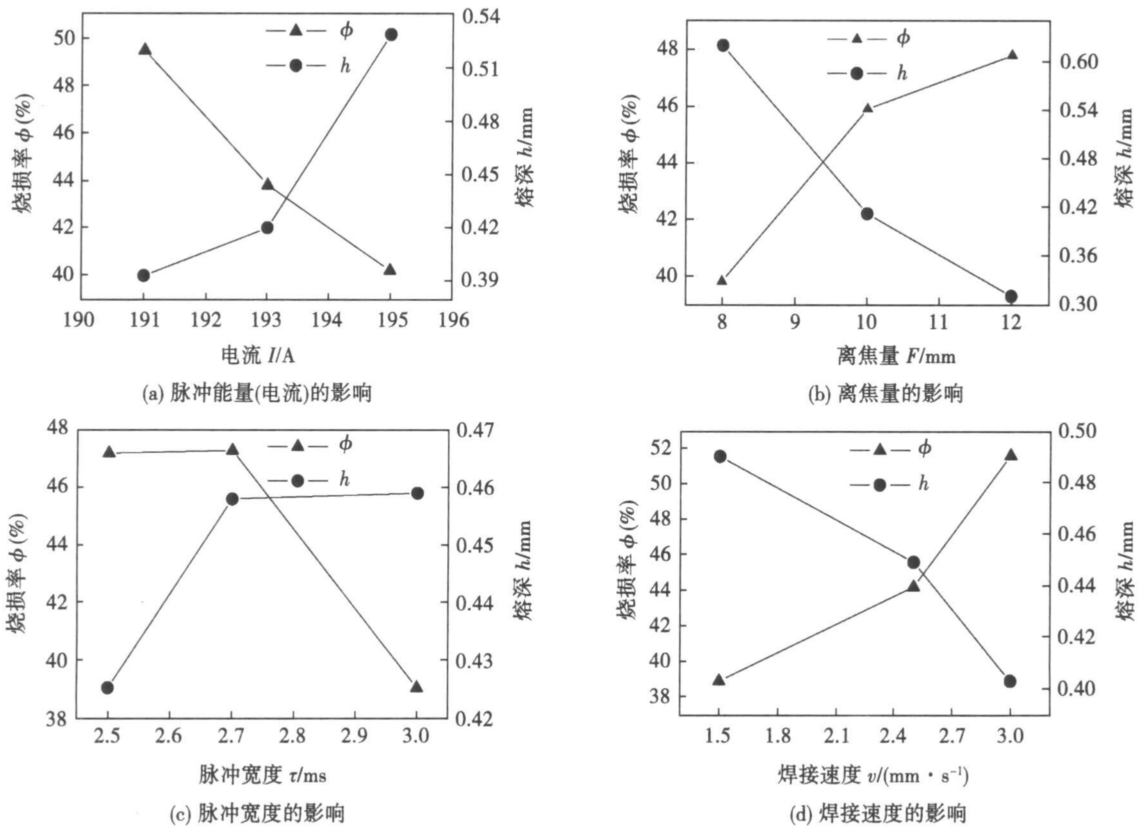

(a) 脉冲能量(电流)的影响　(b) 离焦量的影响

(c) 脉冲宽度的影响　(d) 焊接速度的影响

图 3　焊接参数对烧损率和熔深的影响趋势极差分析

Fig. 3　Influences of welding parameters on weld penetration and evaporation loss of Mg element

由于蒸发是发生在液体表面的汽化过程，故越靠近焊缝表面，Mg元素烧损越多；靠近熔池底部，烧损则较少.

熔池搅拌作用的大小与蒸气压力成正比，而蒸气压力的大小则与激光束的功率密度直接相关．此处，随着反映单脉冲能量大小的电流值增大，脉冲功率密度增大，熔深增大，而且熔池中蒸气压力也随之增大，搅拌作用加强，传质过程加快，Mg元素烧损得以补充，烧损率减少.

随着脉冲宽度增加，脉冲持续时间延长，熔化金属的加热时间延长，液体金属温度升高，蒸发量会有所增加；但脉冲持续时间的延长，也使得熔池中的传质过程得以充分进行，烧损得以补充．当后者起主导作用时，表现为 Mg元素烧损减少.

离焦量影响激光加热斑点的半径以及加热斑点的功率密度．随离焦量增大，聚焦光斑直径增大，加热面积增加，蒸发面积增加，金属蒸发量增加；同时，加热斑点的功率密度减小，表面温度梯度和表面张力梯度减小，熔池金属流动速度变慢，传质过程不能充分进行，烧损的 Mg元素不易补偿，所以烧损率较大.

焊接速度降低时，热输入增加，熔池温度升高，熔深增大．此时，熔池前熔化边沿的液体金属增加，熔池前、后熔化边沿的蒸气压强差和蒸气反作用压强差增大，导致前熔化边沿附近的金属液体向后熔化边沿附近流动，客观上起到了对熔池的搅拌作用．同时，焊接速度降低，使传质过程有充分的进行时间，烧损的 Mg元素得到补充，因此烧损率减少.

2.4　接头显微硬度分析

通过测定 5A05铝合金接头及焊缝的显微硬度来间接反映其力学性能．显微硬度主要受焊缝组织粗细和 Mg元素含量的影响.

图 4为焊接接头的显微硬度分布．由图 4中可看出，熔合线附近硬度最高，焊缝中心和母材的硬度

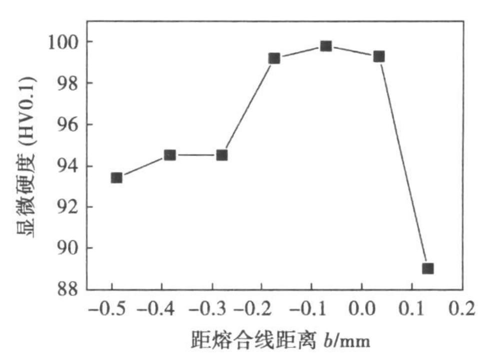

图 4　焊接接头的显微硬度分布

Fig. 4　Micro-hardness distribution of welded joint

较低,焊缝的硬度高于母材. 由于激光是高能密度热源,焊缝金属温度高,焊缝及 HAZ温度梯度大,冷却速度快,使焊缝区晶粒比母材更为细小,这是造成焊缝硬度高于母材的一个重要原因. 熔合线附近的高硬度,除了与细晶组织有关外,还与 Mg元素含量有关. 由于 Mg原子在液态铝中的溶解度大于在固态铝中的溶解度,所以焊接过程中 Mg原子会从固态铝中向液态铝中扩散,且在熔池底部和边缘处 Mg元素的蒸发少,使得熔合线附近的 Mg元素含量高于焊缝中心 (图 2),从而造成了熔合线附近的高硬度.

在焊缝厚度方向从熔池表面到熔池底部硬度先降后增 (图 5). 结合图 2所示的 Mg元素分布可知,虽然从熔池底部到焊缝表面 Mg元素含量有下降趋势,但激光焊缝表面由于受到轴向保护气体的强制冷却作用,使熔池表面冷却速度明显快于中部,从而使焊缝表面组织细化,这样弥补了焊缝由于 Mg元素蒸发烧损引起的硬度下降. 而在焊缝底部,也有较好的散热条件,故有很快的冷却速度,使该部位形成细化的树枝晶,而且此区域的 Mg元素含量较高,因此,焊缝底部硬度再次升高.

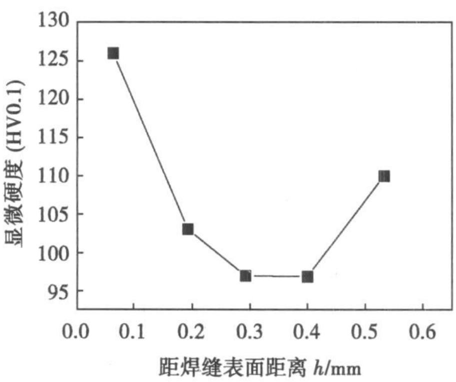

图 5 沿焊缝厚度方向显微硬度分布

Fig. 5 Micro-hardness distribution in depth direction of welded joint

3 结 论

(1)焊缝中 Mg元素的烧损受熔池搅拌作用大小的影响,随搅拌增强,烧损率减小,且随着焊缝深度的增加,烧损程度减少.

(2)在试验条件下,脉冲能量、脉冲宽度、焊接速度和离焦量对 Mg元素烧损率和熔深的影响大体相反. 随着脉冲能量和脉冲宽度的增加,熔深增大,Mg元素烧损率减少;而随着焊接速度和离焦量的增大,熔深减小,Mg元素烧损率增加.

(3)受焊缝 Mg元素含量和组织的影响,熔合线附近硬度较高,焊缝中心和母材的硬度较低,在焊缝厚度方向从熔池表面到熔池底部硬度先降后增.

参考文献:

[1] 张德库, 牛济泰, 于秀宇, 等. 铝基复合材料激光焊工艺参数对焊缝成形和熔深的影响[J]. 哈尔滨工业大学学报, 2002, 34(2): 122-125.
Zhang Deku, Niu Jitai, Yu Xiuyu, et al. Effect of welding parameters on formation and penetration of welds during laser welding of SiC-P/6061 aluminum matrix composites[J]. Journal of Harbin Institute of Technology, 2002, 34(02): 122-125.

[2] Reed C B, Natesan K, Xu Z, et al. The effect of laser welding process parameters on the mechanical and microstructural properties of V-4Cr-4Ti structural materials[J]. Journal of Nuclear Materials, 2000, 28(3): 1206-1209.

[3] Kutsuna M, Suzuki J, Sugiyama S, et al. CO_2 laser welding of A2219, A5083 and A6063 aluminum alloys[J]. Welding in the World, 1993, 31(2): 126-135.

[4] Katayama S, Seto N, Mizutani M, et al. Formation mechanism of porosity in high power YAG laser welding[C] // International Congress on Applications of Lasers and Electro-optics (section C), Dearborn, MI USA, 2000: 16-24.

[5] Matsunawa A, Katayama S. Understanding physical mechanisms in laser welding for construction of mathematical model[J]. Welding in the World, 2002, 46(7): 27-38.

[6] Cicala E, Duffet G, Andrzejewski H, et al. Hot cracking in Al-Mg-Si alloy laser welding operating parameters and their effects[J]. Materials Science and Engineering, 2005, 395(1/2): 1-9.

[7] Debroy T, David S A. Physical processes in fusion welding[J]. Reviews of Modern Physics, 1995, 67(1): 85-112.

作者简介: 牛锐锋, 男, 1960年出生, 硕士, 副教授. 主要从事材料焊接性及其焊接工艺方面的科研和教学工作. 发表论文 10余篇. Email: niurf@xaut.edu.cn

that the ductile fracture characteristics when the content of In exceeded 2%, the dissociation morphology fracture would be emerged which had little influence on the tensile property of the brazed joints. The elements of Ga and In distributed uniformly no segregation in the microstructure of the Ag-Cu-Zn-Sn-3Ga-2In filler metal was observed by SEM, and the significant framework structure was found in the matrix.

Key words: Ag based brazing filler metal; microstructure; Ga; In

Prediction of tensile property of TIG welding joints in GH99 alloy by artificial neural network WANG Qing, NA Yue, SUN Dongli, LIU Yuhong, DENG Dejun, YANG Yuyin (1. School of Materials Science and Engineering, Harbin Institute of Technology, Harbin 150001, China; 2. Beijing Power Generating Machinery Institute, Beijing 100072, China). p77—80

Abstract: Multilayer BP network model based on improved algorithm was established with Matlab 7.0 software to predict the tensile property of TIG welding joints of GH99 superalloy. The input parameters of the model consisted welding current, welding speed, pulse frequency, remelting times, plate thickness, assembly clearance and weld groove. The outputs of the Artificial Neural Network (ANN) model included property parameters such as tensile strength, yield strength and elongation. The calculated results showed that the multilayer BP network model based on improved algorithm could predict the tensile property of TIG welding joints of GH99 superalloy. The calculated values were in good agreement with measured data, and the average relative errors between calculated values and measured data of tensile strength, yield strength and elongation were -0.76%, 1.71% and 2.30% respectively.

Key words: GH99 alloy; TIG welding; artificial neural network; tensile property

Evaporation loss of Mg element in pulsed laser welding of 5A05 aluminum alloy and distribution of micro-hardness of welding joint NIU Ruifeng, LIN Binghua, WANG Yani, YANG Xingfei (School of Materials Science and Engineering, Xi'an University of Technology, Xi'an 710048, China). p81—84

Abstract: 5A05 aluminum alloy plate with the thickness of 1 mm was welded with Nd: YAG laser beam. The effect of welding parameters including pulse energy, pulse duration, welding speed and defocusing distance on the evaporation loss of Mg element, depth of fusion, variation of Mg element content in weld metal and micro-hardness of weld joint were studied and analyzed. The results showed that stirring in molten pool had a significant effect on the evaporation loss of Mg element. With the increase of stirring and the weld penetration, the evaporation loss of Mg element was decreased. Due to the effect of Mg element content and cooling rate, the maximum hardness of weld joint was approximately located at the fusion line. From the surface to the bottom of molten pool, the hardness of weld joint first decrease and then increase.

Key words: pulsed Nd: YAG laser welding; evaporation loss of Mg element; aluminum alloy; micro-hardness

Precise calculation methods of power factor for single-phase alternating current spot welding machine ZHANG Yong, MA Tiejun, HE Youxu, YANG Sihan (Shanxi Key Laboratory of Friction Welding Technologies, Northwestern Polytechnical University, Xi'an 710072, China). p85—88

Abstract: Collaborating with the definition of the power factor for the non-sinusoidal waveform, this paper adopted the Fast Fourier Transformation (FFT) to analyze the spectrum of grid voltage and welding current, considered the influence of current harmonics and their phase shifts on the active power, eventually calculated and obtained the accurate power factor of an alternative current spot welding machine. The results showed good coincidence with the theoretical analysis when the power factor changed with the length of the secondary loop. With the same triggering angle of the silicon-controlled rectifier (SCR), the calculated power factor was smaller than that obtained by the traditional angle θ method, but was identical with the data which was measured by the power system. In conclusion, the proposed method is feasible and effective.

Key words: alternating current spot welding; power factor; frequency-domain analysis

Mechanical and fatigue properties of undermatching butt joints of 10CrNi3MoV steel ZHAO Zhili, YANG Jianguo, LIU Xuesong, FANG Hongyuan (1. School of Materials Science & Engineering, Harbin University of Science and Technology, Harbin 150040, China; 2. State Key Laboratory of Advanced Welding Production Technology, Harbin Institute of Technology, Harbin 150001, China). p89—92

Abstract: Based on the tension and pulse fatigue tests, the influence of mismatch ratio on mechanical performance of undermatching flush butt joints of 10CrNi3MoV steel was studied, and the empirical equations for the relationship between mismatch ratio and fatigue strength (or fatigue life) of joints were built. The results of experiments illustrated that the tensile strength, specific elongation and fatigue strength of flushing butt joints decreased with the decreasing mismatch ratio, and the influence on specific elongation and fatigue strength was obviously higher than that on the tensile strength. The tensile strength and fatigue strength of undermatching flush butt joints exceed their deposited metals by the metallurgic strengthening effect and constrained strength effect on weld metal. Because a low to excess of mismatch ratio welded structure lacking plasticity reserve of need, the preliminary definition of low limit of mismatch ratio was attempted under standard of the rupture models of welded joints.

Key words: undermatching butt joints; mechanical properties; fatigue properties; mismatch ratio

Mechanism of cracks generation in hardfacing pinch roll WANG Qingbao, LI Zhuoxin, SHI Yaowu (1. Department of Materials Science and Engineering, Beijing University of Technology, Beijing 100022, China; 2. MCC Welding Science & Technology Co. Ltd, Beijing 100088, China). p93—96

Abstract: Hot cracks formed in pinch roll frequently after repaired by hardfacing because the material was chosen improperly and low purity. This happened even if the hardfacing tech-